Pergamon

Mechanics Research Communications, Vol. 27, No. 5, pp. 561–566, 2000

0093-6413/00/$–see front matter

PII: S0093-6413(00)00130-0

DYNAMIC BUCKLING OF LAMINATED THICK SHALLOW SPHERICAL CAP BASED ON A STATIC ANALYSIS

G.P.DUBE, P.C.DUMIR and A.MALLICK
Applied Mechanics Department, I.I.T. Delhi, New Delhi-110016, India

(Received 28 February 2000; accepted for print 7August 2000)

Introduction

Shallow spherical caps have wide applications in many structures. The work on buckling of isotropic thin caps is reviewed by Simitses [1]. The nonlinear axisymmetric response of orthotropic thin spherical caps is presented in Refs. [2–5]. The effect of shear deformation should be included for thick caps. Dumir [6] and Dumir and Shingal [7] used orthogonal point collocation method for nonlinear analyses of orthotropic thick caps. Xu [8] and Xu and Chia [9, 10] presented axisymmetric buckling and postbuckling analyses of laminated thick spherical caps using Fourier-Bessel series. Nath and Sandeep [11, 12] used Chebyschev series for static and dynamic buckling analyses of laminated polar orthotropic spherical thick caps. Sathyamoorthy [13, 14] studied nonlinear vibration of thick isotropic and orthotropic spherical caps using Galerkin method.

This paper deals with the axisymmetric dynamic buckling of laminated thick spherical caps with radially orthrotropic layers under uniformly distributed step load. Although this lay-up is presently difficult to manufacture, yet researchers [8-12,15,16] have analysed the behaviour of such lay-ups for possible advantages. Marguerre-type, first order shear deformation theory (FSDT) for moderately thick shallow spherical laminated shell is employed. The solution for the static case is obtained by the orthogonal point collocation method. Based on mechanical energy conservation, an approximate value of the maximun deflection response under step load is obtained from the static analysis. It is assumed that at the instant of the peak average deflection under step load the cap has zero velocity everywhere and its deflected shape is the same as that under a static load which causes the same average deflection. The dynamic buckling load is then determined as the load at which a local maximum occurs in the curve of step load versus maximum average deflection, since beyond that snapthrough occurs with large amplitude of motion. However, if there is a gradual transition from the low to the high range of maximum average deflection with increase in the step load, the buckling load is taken as the load at the lower knee of the step load versus maximum average deflection curve. The lower knee corresponds to the maximum curvature point in the load deflection curve. Beyond this, the amplitude of vibration increases rapidly with the load. Therefore, the load at the lower knee has been taken as the critical load in Refs. [17,18]. The buckling load is also determined using the classical lamination theory (CLT). Symmetrically and unsymmetrically laminated caps, with clamped and simple supports having movable and immovable edge conditions, are analysed. The present economical approach yields quite accurate results. The results are valid provided the buckling mode is axisymmetric for given set of parameters. The buckling mode may not be axisymmetric for relatively deeper shells.

Governing Equations of FSDT and CLT

Consider a shallow laminated spherical cap of base radius a, thickness h and apex rise H with all its polar orthotropic layers having equal thickness. In the first order shear deformation theory (FSDT), the normal and meridional displacements $w(r,z), u(r,z)$ are approximated as:

$$u(r,z) = u^0(r) + z\psi(r), \qquad w(r,z) = w(r), \tag{1}$$

where $w(r), u^0(r)$ are the displacements of the midsurface and ψ is the rotation of its normal. Denoting differentiation by a subscript comma, retaining nonlinearity due to w alone, Marguerre-type strain-displacement relations are given by [5]:

$$\begin{bmatrix} \varepsilon_r \\ \varepsilon_\theta \end{bmatrix} = \varepsilon^0 + z\kappa, \qquad \varepsilon^0 = \begin{bmatrix} u^0_{,r} + 2Hrw_{,r}/a^2 + \frac{1}{2}w^2_{,r} \\ u^0/r \end{bmatrix}, \qquad \kappa = \begin{bmatrix} \psi_{,r} \\ \psi/r \end{bmatrix}, \qquad \gamma_{zr} = \psi + w_{,r} \tag{2}$$

Assuming $\sigma_z \simeq 0$ and the constitutive equation of polar orthotropic layers yields the following expressions for the force resultants $N = [N_r \ N_\theta]^{\mathrm{T}}$, $M = [M_r \ M_\theta]^{\mathrm{T}}$ and Q_r:

$$N = A\varepsilon^0 + B\kappa, \qquad M = B\varepsilon^0 + D\kappa, \qquad Q_r = A_{55}\gamma_{zr}, \qquad \varepsilon^0 = A^*N + B^*\kappa, \qquad M = -B^{*T}N + D^*\kappa, \tag{3}$$

with $[A,B,D] = \int_{-h/2}^{h/2} Q[1,z,z^2]\,\mathrm{d}z$, $A^* = A^{-1}, B^* = -A^{-1}B, D^* = D - BA^{-1}B, A_{55} = k_5^2\int_{-h/2}^{h/2} Q_{55}dz$. The elements of the matrix Q are: $Q_{11} = E_1/(1-\nu_{12}\nu_{21})$, $Q_{12} = \nu_{12}E_2/(1-\nu_{12}\nu_{21})$, $Q_{22} = E_2/(1-\nu_{12}\nu_{21})$, $Q_{55} = G_{31} = G_{zr}$ where E_i are Young's moduli, ν_{ij} are Poisson's ratios and G_{ij} are shear moduli. The factor k_5^2 is the shear correction factor which has been taken as 5/6 in this study. Neglecting inplane inertia, the inplane equilibrium equation, $(rN_r)_{,r}/r - N_\theta/r = 0$, is satisfied by expressing N_r, N_θ in terms of a stress function Φ with $N_r = \Phi/r, N_\theta = \Phi_{,r}$. The equations of rotational and transverse motion are

$$(rM_r)_{,r}/r - M_\theta/r - Q_r = I_2\ddot{\psi}, \qquad (rQ_r)_{,r}/r + [rN_r(w_{,r} + 2Hr/a^2)]_{,r}/r + p_z = I_0\ddot{w}, \tag{4}$$

where p_z is the uniformly distributed load and $(I_0, I_2) = \int_{-h/2}^{h/2}\gamma[1,z^2]dz$, with γ being the mass density.

The various entities are nondimensionalised as follows

$$\begin{gathered} \rho = r/a, \quad \bar{w} = w/h, \quad \bar{u} = ua/h^2, \quad \bar{\psi} = a\psi/h, \quad \bar{\Phi} = a\Phi/E_0h^3, \quad \tau = t(h/a^2)(E_0/\gamma_0)^{1/2}, \\ \bar{A}_{ij} = A_{ij}/E_0h, \quad \bar{B}_{\alpha\beta} = B_{\alpha\beta}/E_0h^2, \quad \bar{D}_{\alpha\beta} = D_{\alpha\beta}/E_0h^3, \quad \bar{A}^*_{\alpha\beta} = A^*_{\alpha\beta}E_0h, \quad \bar{D}^*_{\alpha\beta} = D^*_{\alpha\beta}/E_0h^3, \\ \bar{B}^*_{\alpha\beta} = B^*_{\alpha\beta}/h, \quad s = a/h, \quad Q = (p_za^4/E_0h^4)h^2/H^2, \quad \lambda = H/a, \quad \bar{I}_0 = I_0/\gamma_0h, \quad \bar{I}_2 = I_2/\gamma_0h^3, \end{gathered} \tag{5}$$

where γ_0, E_0 are the density and a specific modulus of a layer. The compatibility equation for strains, viz., $\varepsilon^0_r - (r\varepsilon^0_\theta)_{,r} = w^2_{,r}/2 + 2Hrw_{,r}/a^2$, and equations of motion (4) can be expressed in dimensionless form as:

$$A^*_{22}(\rho\Phi'' + \Phi') - A^*_{11}\Phi/\rho + B^*_{21}\rho\psi'' + (B^*_{21} + B^*_{22} - B^*_{11})\psi' - B^*_{12}\psi/\rho + 2\lambda s\rho w' + w'^2/2 = 0, \tag{6}$$

$$-B^*_{21}\Phi'' - (B^*_{11} + B^*_{21} - B^*_{22})\Phi'/\rho + B^*_{12}\Phi/\rho^2 + D^*_{11}(\psi'' + \psi'/\rho) - D^*_{22}\psi/\rho^2 - A_{55}(\psi + w')s^2 = I_2\ddot{\psi}/s^2, \tag{7}$$

$$s^2A_{55}\rho(\psi + w') + \Phi(w' + 2\lambda s\rho) + \int_0^\rho [s^2\lambda^2Q - I_0\ddot{w}]\rho\, d\rho = 0, \tag{8}$$

where $(\ )' = (\ )_{,\rho}$ and overbar is omitted for simplicity. The governing equations (6) to (8) are identical to those used by Nath and Sandeep [12] based on different strain-displacement relations. For classical lamination theory (CLT), $\psi = -w'$ and the governing equations are the compatibility equation (6) and the equation of motion obtained by forming ρ[eq.(7)] + [eq.(8)] with $\ddot{\psi} = 0$:

$$A^*_{22}(\rho\Phi'' + \Phi') - A^*_{11}\Phi/\rho - B^*_{21}\rho w''' - (B^*_{21} + B^*_{22} - B^*_{11})w'' + B^*_{12}w'/\rho + 2\lambda s\rho w' + w'^2/2 = 0, \tag{9}$$

$$\begin{aligned} -B^*_{21}\rho\Phi'' - (B^*_{11} + B^*_{21} - B^*_{22})\Phi' + B^*_{12}\Phi/\rho - D^*_{11}(\rho w''' + w'') + D^*_{22}w'/\rho - +\Phi(w' + 2\lambda s\rho) \\ + \int_0^\rho [s^2\lambda^2Q - I_0\ddot{w}]\rho\, d\rho = 0, \end{aligned} \tag{10}$$

Clamped (C) and simply-supported (S) caps are considered with movable (M) and immovable (I) inplane boundary condition at $r = a$, i.e., for

$$\begin{array}{llll} \text{FSDT:} & \rho = 1: \quad w = 0, & C: \quad \psi = 0, & S: \quad M_r = -B_{11}^*\Phi - B_{21}^*\Phi' + D_{11}^*\psi' + D_{12}^*\psi = 0 \\ & & M: \quad \Phi = 0, & I: \quad u = A_{21}^*\Phi + A_{22}^*\Phi' + B_{21}^*\psi' + B_{22}^*\psi = 0. \\ & \rho = 0: \quad \psi = 0, & \Phi = 0. & \end{array} \tag{11}$$

$$\begin{array}{llll} \text{CLT:} & \rho = 1: \quad w = 0, & C: \quad w' = 0, & S: \quad M_r = -B_{11}^*\Phi - B_{21}^*\Phi' - D_{11}^*w'' - D_{12}^*w' = 0 \\ & & M: \quad \Phi = 0, & I: \quad u = A_{21}^*\Phi + A_{22}^*\Phi' - B_{21}^*w'' - B_{22}^*w' = 0. \\ & \rho = 0: \quad w' = 0, & \Phi = 0. & \end{array} \tag{12}$$

Method of Solution

A static analysis for uniformly distributed load Q is performed. The marching variable, the average deflection $w_{\mathrm{av}} = 2\int_0^1 w\rho\, d\rho$, is incremented in small steps. The orthogonal point collocation method [7] is used to solve the nonlinear equations (6)–(8) of FSDT with inertia terms as zero. Since w, ψ and Φ have to satisfy, respectively, 1, 2 and 2 boundary conditions, these are approximated at the kth step by expanding as finite degree polynomials in ρ:

$$w = \sum_{j=1}^{N+1} \rho^{j-1} a_j, \qquad \psi = \sum_{j=1}^{N+2} \rho^{j-1} b_j, \qquad \Phi = \sum_{j=1}^{N+2} \rho^{j-1} c_j, \tag{13}$$

where N is the number of collocation points ρ_i, $i = 1, \ldots, N$. The collocation points ρ_i are taken at the zeros of Nth degree Legendre polynomial. The discretised equations are solved iteratively by the Newton-Raphson method. For the first iteration, the predicted values a_{j_p}, b_{j_p}, c_{j_p} of a_j, b_j, c_j at kth step are extrapolated from the values at the three preceding steps; e.g.,

$$a_{j_p} = A_1 a_{j_{k-1}} + A_2 a_{j_{k-2}} + A_3 a_{j_{k-3}} \tag{14}$$

with $A_1, A_2, A_3 = 1, 0, 0$ ($k = 1$); $2, -1, 0$ ($k = 2$); $3, -3, 1$ ($k \geq 3$). and a subscript k denotes the value at the kth step. For the current iteration a_j, b_j, c_j are updated as

$$a_j = a_{j_p} + \Delta a_j, \qquad b_j = b_{j_p} + \Delta b_j, \qquad c_j = c_{j_p} + \Delta c_j, \tag{15}$$

These are substituted in the three governing differential equations (6)–(8) and the equations are linearised for the unknowns $\Delta a_j, \Delta b_j, \Delta c_j$. The $3N$ collocation equations ($i = 1, 2, \ldots, N$) for these linearised equations, the five boundary conditions (11) and an equation for the average deflection yield $3N+6$ algebraic equations. These equations are not listed for brevity. These equations are solved for $\Delta a_j, \Delta b_j, \Delta c_j$ and the applied load Q. The iterations are stopped when the difference between the values of $Q, \Phi'(0), \Phi'(1), w'(0.5), \psi(0.5)$ at successive iterations is less than 0.001%. For CLT, w and Φ are expanded in terms of $N+3$ and $N+2$ terms. The coefficients in their expansion are obtained using $2N$ collocation equations for the compatibility equation (9) and the transverse equilibrium equation (10) and five boundary conditions (12).

An approximate value of the maximum average deflection response $w_{\mathrm{av}_{\max}}$ under step load is also predicted from the static analysis. It is assumed that at the instant of the maximum value of the average deflection response, the whole of cap has zero velocity and the deflected shape is the same as that under a static load which causes the same value of the average deflection. If a static uniformly distributed load Q results in an average deflection w_{av} with the strain energy $U(Q)$, then the step load Q_0 (p_{z_0}) which will yield the maximum average deflection $w_{\mathrm{av}_{\max}}$ equal to w_{av} is obtained from the equation of energy balance

$$\int_0^a w(r) p_{z_0} 2\pi r\, dr = 2\pi \Big[\sum_{j=1}^{N+1} a_j/(j+1)\Big] Q_0 E_0 h^3 H^2/a^2 = U(Q) \tag{16}$$

The strain energy $U(Q)$ for the static load is obtained using the static solution for w, Φ, ψ. For FSDT, the strain energy U of the shell is given by

$$U = \int_A \int_{-h/2}^{h/2} \frac{1}{2}[\sigma_r \varepsilon_r + \sigma_\theta \varepsilon_\theta + \gamma_{zr}\tau_{zr}]dzdA = \frac{1}{2}\int_A \int_{-h/2}^{h/2}[\sigma_r(\varepsilon_r^0 + z\kappa_r) + \sigma_\theta(\varepsilon_\theta^0 + z\kappa_\theta) + \gamma_{zr}\tau_{zr}]dzdA$$
$$= \int_b^a [N_r\varepsilon_r^0 + M_r\kappa_r + N_\theta\varepsilon_\theta^0 + M_\theta\kappa_\theta + Q_r(\psi + w_{,r})]\pi r\, dr \tag{17}$$

The strain energy $U(Q)$ for static load Q can be expressed in terms of the static solution for w, Φ, ψ as

$$U(a-b)^2/E_0h^5 = \pi \int_0^1 [\bar{A}_{11}^*\bar{\Phi}^2/\rho^2 + \bar{A}_{22}^*\bar{\Phi}'^2 + 2\bar{A}_{12}^*\bar{\Phi}\bar{\Phi}'/\rho + \bar{D}_{11}^*\bar{\psi}'^2 + \bar{D}_{22}^*\bar{\psi}^2/\rho^2 + 2\bar{D}_{12}^*\bar{\psi}\bar{\psi}'/\rho$$
$$+s^2\bar{A}_{55}(\bar{\psi} + \bar{w}')^2]\rho\, d\rho \tag{18}$$

For CLT, $U(Q)$ for static load Q can be expressed in terms of the corresponding static solution for w, Φ as

$$U(a-b)^2/E_0h^5 = \pi \int_0^1 [\bar{A}_{11}^*\bar{\Phi}^2/\rho^2 + \bar{A}_{22}^*\bar{\Phi}'^2 + 2\bar{A}_{12}^*\bar{\Phi}\bar{\Phi}'/\rho + \bar{D}_{11}^*\bar{w}''^2 + \bar{D}_{22}^*\bar{w}'^2/\rho^2 + 2\bar{D}_{12}^*\bar{w}'\bar{w}''/\rho]\rho\, d\rho \tag{19}$$

Results and Discussion

The material properties of graphite-epoxy (Gr/Ep), boron-epoxy (Bo/Ep) and glass-epoxy (Gl/Ep) composite are taken as $E_1/E_2 = 40, 10, 3$; $G_{31}/E_2 = G_{32}/E_2 = 0.5, 0.33, 0.5, \nu_{12} = 0.25, 0.22, 0.25$, respectively. The modulus E_0 for nondimensionalisation has been taken as $E_0 = E_2$. Convergence studies, have revealed that very good accuracy is achieved for ten collocation points. A ply is termed a 0° ply or a 90° ply if the greater Young's modulus is in the radial or circumferential direction, respectively.

The deflection response w_{av} of 6-ply (90°/0°/90°/0°/90°/0°) immovable simply-supported Gr/Ep caps with $H/a = 0.2, a/h = 10$ under static load Q is shown in fig. 1. The approximate value of maximum average deflection $w_{\mathrm{av_{max}}}$ under step load Q_0, predicted from static solution, is also depicted in this figure. The predicted value of dynamic buckling load for FSDT obtained from a single static response curve, indicated as Q_{cr} in fig. 1, corresponds to the local maximum of the Q_0–$w_{\mathrm{av_{max}}}$ curve if such a maxima exists. It is the value of the step load at which the cap snaps through and oscillates about the opposite undeformed configuration of the cap. However, if there is a gradual transition from the low to the high range of maximum average deflection with increase in the step load, then the buckling load is taken as the load corresponding to the lower knee of the step load versus maximum average deflection curve as shown in fig. 1 for the case of 5-ply (90°/0°/90°/0°/90°/0°) clamped immovable Gr/Ep cap with $H/a = 0.15, a/h = 10$. Nath and Sandeep [12] have obtained the value of dynamic buckling load by performing several dynamic analyses for several values of the step load. The dynamic buckling load of clamped immovable 5-ply (90°/0°/90°/0°/90°) Gr/Ep caps with $a/h = 10$, obtained by the present static approach, is presented in fig. 2. It is observed that the present results agree well with the results of Nath and Sandeep [12] obtained by dynamic analyses. Similar comparisons for simply-supported immovable 6-ply (90°/0°/90°/0°/90°/0°) caps with different values of a/h and material properties are presented in figs. 3 and 4. The present results agree very well with the results of Nath and Sandeep [12]. The dynamic buckling load of simply-supported movable and clamped movable, 5-ply (0°/90°/0°/90°/0°) Gr/Ep caps, obtained by static and dynamic analyses, is shown in figs. 5 and 6. There is good agreement among these results obtained by static and dynamic analysis.

Conclusions

Dynamic buckling analysis is presented for thick laminated spherical cap under uniformly distributed load using FSDT and CLT. Dynamic buckling load is predicted by using mechanical energy conservation to obtain approximate maximum deflection response under step load from static response analysis. The accuracy of the present economical approach is quite good for various values of the thickness parameter and shell parameter for clamped and simply-supported caps with immovable and movable inplane boundary conditions for symmetrical as well as antisymmetrical laminations.

References

1. G.J. Simitses, Dynamic stability of suddenly loaded structures, Springer-Verlag, New York (1990)
2. T.K. Vardan, ASME J. Appl. Mech. **45**, 445 (1978)
3. T.K. Vardan and K.A.V. Pandalai, Comput. Struct. **9**, 417 (1978)
4. P.C. Dumir, Y. Nath and M.L. Gandhi, Int. J. Sci. Eng. **1**, 67 (1984)
5. P.C. Dumir, M.L. Gandhi and Y. Nath, Acta Mech. **52**, 93 (1984)
6. P.C. Dumir, Ingenieur-Archive **55**, 277 (1985)
7. P.C. Dumir and L. Shingal, Arab. J. Sci. and Engg. **11**, 298 (1986)
8. C. Xu, Int. J. Solids and Struc. **28**, 1171 (1991)
9. C. Xu and C.Y. Chia, Int. J. Nonlin. Mech. **29**, 247 (1994)
10. C. Xu and C.Y. Chia, Composites Sci. Tech. **54**, 62 (1995)
11. Y. Nath and K. Sandeep, Int. J. Mech. Sci. **35**, 965 (1993)
12. Y. Nath and K. Sandeep, Composite Structures **40**, 67 (1998)
13. M. Sathyamoorthy, J. Sound and Vib. **172**, 63 (1994)
14. M. Sathyamoorthy, Computers and Structures **57**, 59 (1995)
15. R.S. Alwar and M.C. Narsimhann, Int. J. Nonlinear Mech. **27**, 611 (1992)
16. R.H. Liu, Applied Math. Mech. **12**, 271 (1991)
17. R. Kao and N. Perrone, Computers and Structures **9**, 463 (1978)
18. W.B. Stephens and R.E. Fulton, AIAA Journal **7**, 2120 (1969)

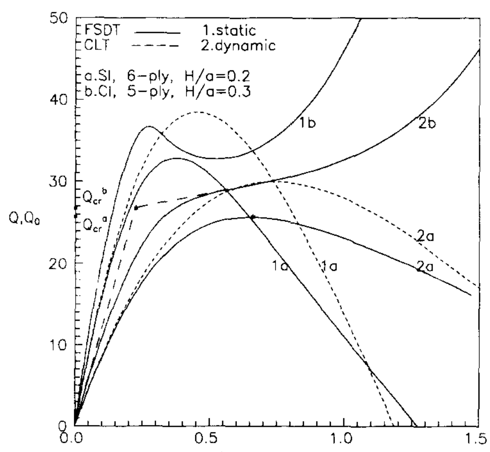

FIG. 1

Response of Gr/Ep cap for static and step load

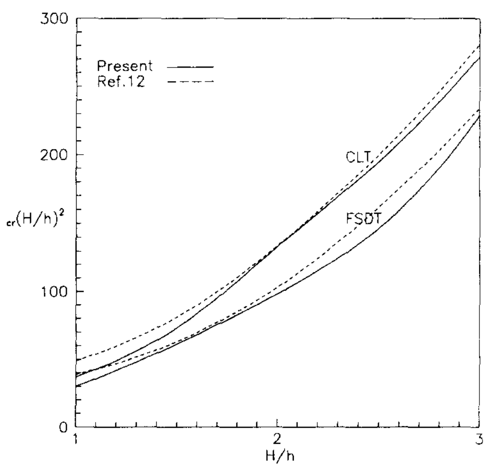

FIG. 2

Q_{cr} of CI 5-ply, Gr/Ep cap, $a/h = 10$

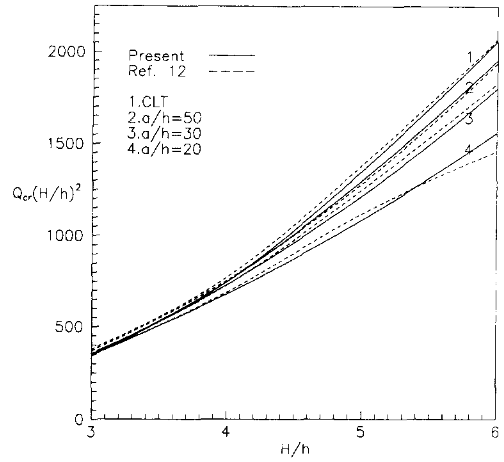

FIG. 3

Q_{cr} of SI 6-ply, Gr/Ep cap

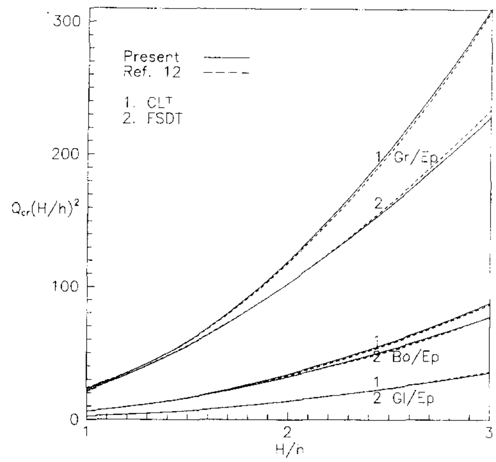

FIG. 4

Q_{cr} of SI 6-ply cap, $a/h = 10$

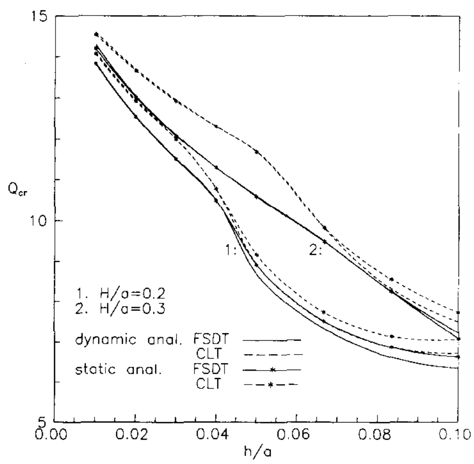

FIG. 5

Q_{cr} of SM 5-ply, Gr/Ep cap

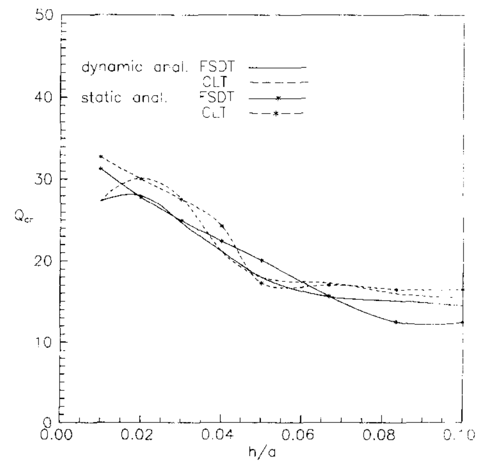

FIG. 6

Q_{cr} of CM 5-ply, Gr/Ep cap,